Direct Structural Observation of an Acyl-Enzyme Intermediate in the Hydrolysis of an Ester Substrate by Elastase[†,‡]

Xiaochun Ding, Bjarne F. Rasmussen,[§] Gregory A. Petsko, and Dagmar Ringe[*]

Departments of Biochemistry and Chemistry and Rosenstiel Basic Medical Sciences Research Center, Brandeis University, Waltham, Massachusetts 02254

Received January 24, 1994; Revised Manuscript Received May 31, 1994[⊕]

ABSTRACT: The method of X-ray crystallographic cryoenzymology has been used to determine the crystal structure of a kinetically significant species on the reaction pathway of a crystalline enzyme. The structure of a specific acyl-enzyme intermediate in the elastase-catalyzed hydrolysis of the *N*-carbobenzoxy-L-alanine *p*-nitrophenyl ester has been determined and refined against X-ray diffraction data at 2.3-Å resolution. The difference Fourier electron density map clearly shows electron density for the trapped acyl-enzyme. The acyl-enzyme was formed at −26 °C and was stabilized at −55 °C during data collection, taking advantage of the glass transition in protein dynamics that occurs at around −50 °C.

Central to the hypothesis for the mechanism of serine proteases is the existence of the covalent acyl-enzyme intermediate. This intermediate was initially invoked to interpret the observation of an initial burst during the hydrolysis of *p*-nitrophenyl esters by α-chymotrypsin (Hartley & Kilby, 1954). This observation, together with structural, chemical, and other kinetic data (Bender & Kilheffer, 1973; Blow, 1976; Kraut, 1977; Huber & Bode, 1978; James et al. 1980), led to the presently accepted mechanism (Figure 1) for the serine protease catalyzed cleavage of peptide and ester bonds. The first step involves the association of the substrate, RCOX, with the enzyme to form a noncovalent E·S complex, with substrate bound in a productive mode. The peptide carbonyl group is then attacked by the active site serine, with formation of a tetrahedral intermediate. Departure of the leaving group as HX leaves the acyl-enzyme intermediate. Deacylation is the microscopic reverse of these acylation steps, with water as the attacking nucleophile.

Several crystal structures of acyl-serine protease derivatives have been determined. However, in each case, the derivative is stable to hydrolysis. The reactions proceed as far as the acyl-enzyme and no further due to various factors and are therefore considered nonproductive in terms of the mechanism given in Figure 1. For instance, the structure of the acyl-enzyme formed by the reaction of (indolylacryloyl)imidazole with chymotrypsin at pH 4 has been determined. The derivative is not susceptible to hydrolysis, presumably because the enzyme is inactive at this pH, and the carbonyl oxygen is directed away from the oxyanion hole (Henderson, 1970). This same principle, the inability to stabilize the tetrahedral intermediate during hydrolysis because the carbonyl oxygen points away from the oxyanion hole, was used to develop inhibitors for serine proteases (Turner et al., 1987). The structures of the acyl-enzymes formed between chymotrypsin and two of these compounds, *o*-hydroxy-α-methylcinnamic acid *p*-nitrophenyl ester and its *p*-diethylamino derivative, were determined and showed that incorrect positioning of the carbonyl oxygen relative to the oxyanion hole did indeed occur (Stoddard et al., 1990). These structures were obtained at pH 7.4, where the enzyme is normally active, and therefore the lack of deacylation must be due to the incorrect position of the carbonyl oxygen. Another example of an acyl-chymotrypsin derivative is that formed by reaction of the enzyme with 3-benzyl-6-choropyrone at pH 5.6 (Ringe et al., 1986). The structure shows the ester carbonyl oxygen perfectly hydrogen bonded in the oxyanion hole. However, at this pH the histidine is expected to be protonated, and this form of the histidine is stabilized by a salt bridge to the inhibitor. This salt bridge prevents a water molecule from interacting with histidine in order to attack the serine ester linkage.

In a study of inhibitors interacting with *Streptomyces griseus* protease A, James et al. (1980) suggested that the chemical nature of the ester linkage is crucial to further reactivity. They suggest that the acyl-enzyme is a high-energy ester with a pyramidal carbonyl carbon atom, rather than a planar carbonyl carbon atom, with the oxygen remaining in the strongly polarizing electrostatic field of the oxyanion hole. The electronic strain accumulated in the acyl-enzyme is then released in the subsequent reaction, forming the tetrahedral product intermediate.

So far, the structures of acyl-enzyme complexes observed crystallographically have been nonproductive in terms of substrate turnover. It would be nice to see a productive intermediate in an actual enzyme reaction pathway structurally. If direct structural observation of a productive intermediate in an enzyme reaction pathway is not possible under normal conditions, it may be possible to trap such an intermediate either by extremely fast data acquisition or by taking advantage of the kinetic parameters that control the formation and breakdown of the intermediate. Even extremely fast data acquisition techniques, such as Laue diffraction (Ringe et al., 1992), may not be successful in obtaining the structures of such intermediates because, in general, intermediates are present in low concentrations and are too short-lived even for this technique. For instance, Bartunik et al. (1992) reported a crystallographic experiment in which the productive substrate Boc-Pro-Ala-Ala-OMe was diffused into crystals of elastase at −53 °C, followed by slow raising of the

[†] Supported by a grant from the National Institutes of Health (GM-26788) and (in part) by a grant from the Lucille P. Markey Charitable Trust.

[‡] Coordinates for native elastase at −45 °C and for the acyl-enzyme at −55 °C have been deposited with the PDB and are available under entry numbers 1ESA and 1ESB.

[*] Corresponding author.

[§] Present address: c/o I.L.L. B.P. 156X, 38042 Grenoble Cedex 9, France.

[⊕] Abstract published in *Advance ACS Abstracts*, July 15, 1994.

0006-2960/94/0433-9285$04.50/0

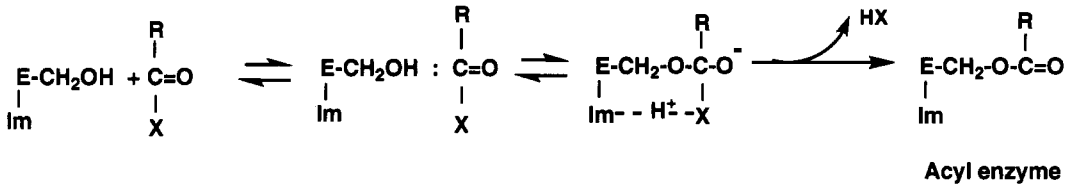

FIGURE 1: Proposed mechanism for the serine proteases (James et al., 1980). Only the acylation step is shown. E represents enzyme, CH_2OH represents the hydroxyl of Ser 203(195), Im represents the imidazole of His 57, and RCOX represents substrate, which can be a peptide, ester, or amide. Deacylation is the microscopic reverse of these acylation steps, with water as the attacking nucleophile.

temperature. The data obtained at −29 and −9 °C were interpreted as a mixture of the Michaelis complex and the acyl-enzyme coexisting simultaneously on the enzyme.

Therefore, accumulation of an intermediate at low temperature, taking advantage of an activation energy barrier for the breakdown of that intermediate, would seem to be the best method to obtain structural data. Previous solution experiments (Fink & Ahmed, 1976) indicate that an acyl-enzyme complex formed from the reaction of elastase with substrate *N*-carbobenzoxy-L-alanine-*p*-nitrophenyl ester (ZAP) accumulates to an occupancy of over 80% at a temperature below −37 °C and that the intermediate breaks down at a sufficiently slow rate (deacylation rate < 10^{-12} mol s^{-1}) that crystallographic data collection is possible. A structural study aimed at obtaining such data was reported with elastase and the substrate ZAP (Alber et al., 1976). The acyl-enzyme complex was generated and trapped at a nominal temperature of −55 °C and a structure determined. Unfortunately, the crystal only diffracted to 3.5-Å resolution, in part due to cracking of the crystals, and therefore a high-resolution view of the intermediate was not possible.

In the experiments reported in this paper, the objective was to generate the productive acyl-enzyme intermediate at a temperature at which it can accumulate and then stabilize the complex by dropping the temperature so that it cannot deacylate. This novel approach to stabilizing transient enzyme-bound species is based upon recent observations of a glasslike transition in the dynamic properties of proteins at around −50 °C (Morozov & Gevorkian et al., 1985; Frauenfelder & Gratton et al., 1986; Parak, 1986; Iben et al., 1989; Doster et al., 1986, 1989, 1991; Goldanskii et al., 1989; Champion, 1992). Crystallographic studies on ribonuclease A have shown that substrates and inhibitors can bind rapidly to the crystalline enzyme at temperatures above this transition, but that binding or dissociation of bound species occurs extremely slowly (Rasmussen et al., 1992) below the transition. Therefore, if an enzyme-bound intermediate is allowed to accumulate in the crystal at a temperature that is above the transition temperature, it may be stabilized for very long periods of time if the temperature is suddenly dropped below the "glass" transition point.

MATERIALS AND METHODS

Porcine pancreatic elastase (PPE) was purchased from Worthington Biochemical and was used without further purification. Crystals were grown by the vapor diffusion sitting drop method, using published crystallization conditions (Sawyer et al., 1978) that were adjusted as needed.

Substrates *N*-carbobenzoxy-L-alanine *p*-nitrophenyl ester (ZAP) and *N*-[3-(2-furyl)acryloyl]-L-leucine methyl ester (Fa-Leu-OMe) were purchased from Sigma Chemical and were used without further purification. The K_M for Fa-LeuOMe was measured by the procedure of Geneste et al. (1969). The hydrolysis of Fa-Leu-OMe was followed at 340 nm.

Table 1: Solutions for Transferring Crystals[a]

solution	[NaAc] (mM)	[Na_2SO_4] (mM)	MeOH (%, v/v)	proton activity
S0	10	10		5.0
S1	10	1		5.0
S2	10	1	10	5.0
S3	10	1	20	5.0
S4	10	1	40	5.0
S5	10	1	50	5.6
S6	10	1	56	6.0
S7	10	1	60	6.3
S8	10	1	64	6.4
S9	10	1	70	6.7

[a] The mother liquor in which the crystals are maintained was slowly changed from the crystallization solution (S0) to the solution used for the trapping experiments (S9). Crystals remained in one solution for 15 min before being transferred to the next. All transfers were done at 4 °C.

Cryoprotection of the Elastase Crystal. Petsko (1975) has discussed the determination of suitable cryoprotective mother liquors for crystalline proteins in detail, and further considerations about the methodology for cryoprotection of protein crystals have been described (Douzou & Petsko, 1984). The critical considerations in the transfer of protein crystals to mixed solvents are to keep the dielectric constant of the medium as near as possible to the value for the normal mother liquor and to ensure that the proton activity does not change too much in any one transfer. Elastase crystals were grown from sodium sulfate–sodium acetate solutions at low ionic strength and pH 5.0. The crystals cannot be transferred directly from the crystallization mother liquor to an alcohol–water mixture because of the low solubility of sodium sulfate in alcohol. During transfer experiments, we also found that elastase crystals become disordered in totally sodium sulfate free solutions. Therefore, 1 mM sodium sulfate is kept in all transfer solutions, since 1 mM sodium sulfate does not precipitate out of a 70% methanol–30% aqueous solution down to −60 °C. We were able to move elastase crystals successfully from an aqueous solution containing 10 mM sodium acetate and 10 mM sodium sulfate at pH 5.0 to a 70% methanol–30% aqueous solution containing 10 mM sodium acetate (v/v) and 1 mM sodium sulfate at a proton activity of 6.7. This transfer was only possible at 4 °C in a stepwise fashion following the procedure in Table 1. Crystals stayed in any one solution for about 15 min before they were moved to the following solution.

Substrate Binding, Data Collection, and Data Processing. (1) Formation of the Acyl-Enzyme at −26 °C Followed by Trapping at −55 °C in 70% MeOH. A crystal of elastase was mounted in a flow cell, allowing substrate to flow through the crystal continuously. The crystal was bathed in 70% MeOH–30% aqueous solution containing 10 mM sodium acetate and 1 mM sodium sulfate at a proton activity (pH*) of 6.7. This solution is a cryoprotective mother liquor that does not freeze down to −85 °C, has low viscosity so that diffusion is rapid, and is known to maintain the activity of the enzyme both in solution and in the crystalline state (Fink & Ahmed, 1976).

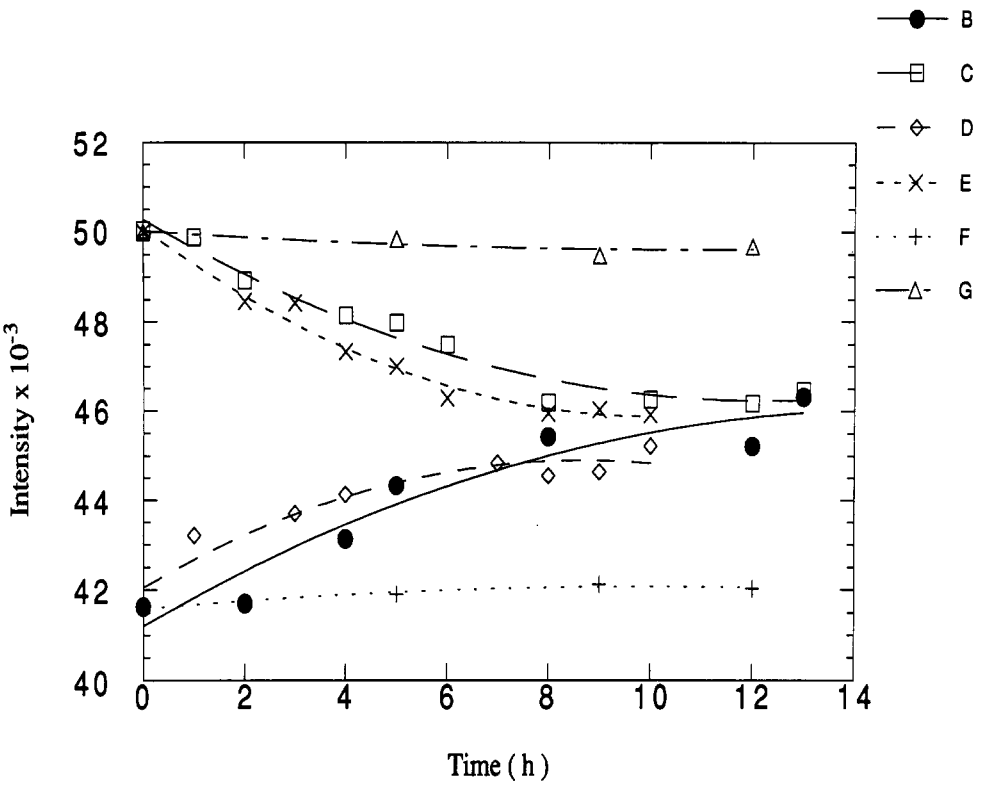

FIGURE 2: Plots of the changes in intensity with time of two high-resolution 0*kl* reflections of elastase as substrate is added: B and C, elastase + ZAP at –26 °C, 70% MeOH–30% aqueous buffer; D and E, elastase + Fa-Leu-OMe at –26 °C, 56% MeOH–44% aqueous buffer; F and G, elastase + Fa-Leu-OMe at –45 °C, 56% MeOH–44% aqueous buffer). The reflection for B, D, and F is the [0, 12, 4]. The intensities were normalized to the intensity of this reflection at time 0. All of these intensities were normalized to each other. The reflection for C, E, and G is the [0, 10, 11]. These intensities were normalized the same as for B, D, and F.

The flow cell was mounted on a Siemens P3 single-counter four-circle diffractometer equipped with a modified LT-1 low-temperature device and a cryostat designed and constructed specifically for this project.

The substrate chosen for this study was ZAP, as it was the substrate about which the most kinetic information was available (Fink & Ahmed, 1976). It is a small substrate with a reasonable ratio of solubility in cryosolvent relative to K_M (k_{cat}/K_M is reported as 185×10^3 M^{-1} s^{-1}; K_M was estimated as 0.6 mM) (Geneste & Bender, 1969). It was dissolved in a solution containing 70% methanol, 10 mM sodium acetate, and 1 mM sodium sulfate (pH* 6.7) at a final concentration of 3.0 mM. To avoid problems due to spontaneous hydrolysis, the solution was made fresh twice daily.

The crystal of elastase in the flow cell/cryostat system was first cooled to –26 °C. For substrate binding at –26 °C, a flow rate of about 10 mL day^{-1} was used. A small set of medium-intensity reflections at high resolution was measured at regular intervals. Time-dependent intensity changes were observed and used to monitor binding. After the binding monitor curve had leveled off (Figure 2), the crystal was cooled to –55 °C to stabilize the expected covalent acyl-enzyme intermediate against further breakdown (Rasmussen et al., 1992), and a complete set of crystallographic data to 2.3-Å resolution was collected using the background–peak–background ω-scan method. Absorption, linear radiation decay, and Lorentz polarization corrections were applied. All reflections with intensity $I/\sigma(I) > 1$ were included. Data completeness is 97%. Initial refinement was carried out with the program PROLSQ (Hendrickson & Konnert, 1978; Konnert & Hendrickson, 1980). The initial phases were calculated using the coordinates of native elastase to 1.65 Å in 56% MeOH at –45 °C, from which all solvent molecules were removed (vide infra). These coordinates were used in order to obtain a more accurate comparison between native enzyme and substrate-bound enzyme. These phases, together with the data from 10- to 3-Å resolution, gave an initial model with an overall starting *R*-factor of 39.9%. After the first 19 cycles of refinement, the resolution of the data was extended from 10- to 2.3-Å resolution, and the overall *R*-factor dropped to 30.3%. A difference Fourier electron density map with coefficients $2|F_o| - |F_c|$ was calculated and showed that the model of the protein fit the electron density very well. There was clear electron density in the active site contiguous with the electron density of the Oγ of Ser 203(195),[1] indicating a covalent derivative of the enzyme. There was no density that could be interpreted as a *p*-nitrophenolate leaving group. At the same time, a difference Fourier electron density map with coefficients $|F_o| - |F_c|$ was calculated. In this map, the water molecules and ions that were previously excluded from the initial model were located. Water molecules with electron density at the 3σ level or better were retained, except solvent molecules in the native structure that were within about 3 Å of the active site. The structural calcium and a bound sulfate ion were added. Refinement was continued with data from 10- to 2.3-Å resolution. After another 12 cycles of refinement, the *R*-factor dropped to 24.9%. At this stage, a difference Fourier electron density map with coefficients $2|F_o| - |F_c|$ was calculated. The electron density for the covalently bound species was clear enough to build in the substrate. An energy-minimized initial model for substrate was built using QUANTA (Molecular Simulations Inc.) An Evans & Sutherland PS300 graphics system and the program FRODO

[1] Ser 203 is the active site serine of PPE. The equivalent residues in chymotrypsinogen are given in parentheses. Thus, Ser 203 (195) corresponds to Ser 195 in chymotrypsinogen.

Table 2: Data Collection and Refinement Statistics for Structures of PPE with and without Substrate/Inhibitor

	sample				
	native	with Fa-Leu-OMe	with TFA-Lys-Phe-Iso	with Fa-Leu-OMe	with ZAP
Crystal Environment					
substrate/inhibitor (concn)		Fa-Leu-OMe (15 mM)	TFA-Lys-Phe-Iso (10^{-5} M)	Fa-Leu-OMe (15 mM)	ZAP (3 mM)
reaction temp (°C)		−45	−45	−26	−26
data collection temp (°C)	−45	−45	−45	−26	−55
cryosolvent	56% MeOH–44% aqueous buffer	56% MeOH–44% aqueous buffer	56% MeOH–44% aqueous buffer	56% MeOH–44% aqueous buffer	70% MeOH–30% aqueous buffer
Results					
do intensities of monitored reflections change?		no	no	yes	yes
is there electron density for ligand in the final difference Fourier map?		no	no	no	yes
Data Collection					
space group	*P*212121	*P*212121	*P*212121	*P*212121	*P*212121
unit cell (Å)	$a = 51.37, b = 58.21, c = 74.83, \alpha = \beta = \gamma = 90°$	$a = 51.37, b = 58.21, c = 74.83, \alpha = \beta = \gamma = 90°$	$a = 51.37, b = 58.21, c = 74.83, \alpha = \beta = \gamma = 90°$	$a = 52.27, b = 57.77, c = 75.02, \alpha = \beta = \gamma = 90°$	$a = 52.02, b = 58.12, c = 74.66, \alpha = \beta = \gamma = 90°$
molecules per asymmetric unit	1	1	1	1	1
resolution (Å)	23–1.65	17–1.65	17–1.65	17–2.0	11–2.3
effective resolution[a] (Å)	1.96	2.1	1.85	2.3	2.3
total no. reflections	18435	12129	16498	7694	10437
no. reflections to effective resolution	16146	10028	15516	6504	10437
completness (to effective resolution) (%)	95	74	79	62	97
Refinement Statics					
resolution range (Å)	10–1.65	10–1.65	10–1.65	10–2.0	10–2.3
R-factor ($= \sum\|\|F_o - F_c\|\|/\sum\|F_o\|$)	0.19	0.16	0.20	0.15	0.21
restraints (rms observed)					
bond length (Å)	0.014	0.015	0.015	0.015	0.018
bond angles (deg)	2.6	3.0	3.0	3.0	3.0
average *B*-factor					
main chain	10.6	12.0	14.6	12.4	10.6
side chain	13.6	15.1	17.6	15.9	13.5
water	22.9	25.1	27.6	25.6	20.4
substrate					30.8
total no. of protein atoms	1822	1822	1822	1822	1822
total no. of waters	134	134	134	134	126
total no. of substrate atoms					15

[a] Effective resolution means that the data completeness in the outer resolution shell is larger than 50%.

(Sack, 1988) were used for the modeling of substrate into the difference Fourier electron density at the active site. Further refinement was continued with XPLOR (Brünger et al., 1987; Brünger, 1988) using individual *B*-factors. Most of the ordered water molecules observed in the structure of the acyl-enzyme were found to be close to their corresponding positions in the native structure. Additional water molecules were found using the program WATERHUNTER (Sugio, unpublished) and checked in difference Fourier electron density maps. In total, 126 ordered water molecules were included. The final *R*-factor is 0.21 with good geometry. The final refinement results are given in Table 2.

(2) Native Elastase Data Collection and Refinement. A native elastase structure at −45 °C was determined in order to ensure that no protein conformational change occurs at low temperature. Native elastase data were measured to 1.65-Å resolution in 56% MeOH at −45 °C from a sorted list of intensities, with more counting time spent on the weaker reflections. The background intensities on both sides of the scan were determined using a block of reflections that covered the whole resolution range to correct for any errors in the background during data processing. Another block of reflections covering the complete resolution range was measured at the beginning and end of data collection to correct for decay. PROLSQ (Hendrickson & Konnert, 1978; Konnert & Hendrickson, 1980) and XPLOR (Brünger et al., 1987; Brünger, 1988) were used in refinement as described above. Initial phases were calculated from coordinates taken from Protein Data Bank entry pdb3est.ent (Bernstein et al., 1977), using a structure determination by Meyer et al. (1987) from which all solvent molecules were removed. These phases, together with the data from 10- to 2-Å resolution, gave an initial model with an overall starting *R*-factor of 40.7%. Subsequent cycles of refinement and rebuilding included data to 1.65-Å resolution and led to an *R*-factor of 26.1%. The water molecules and ions that previously were excluded from the initial model were checked in the difference Fourier electron density map with coefficients $|F_o| - |F_c|$. Only water molecules with electron density at the 3σ level or better were retained. Additional water molecules were found using the program WATERHUNTER (Sugio, unpublished) and checked in difference Fourier electron density maps. Further refinement was continued with XPLOR (Brünger et al., 1987, 1988) using individual isotropic *B*-factors. In total, 134 ordered water molecules were included. The final *R*-factor is 0.19 with good geometry. The final refinement results are given in Table 2.

(3) Attempted Formation of the Acyl-Enzyme at −45 °C in 56% MeOH. The substrate *N*-[3-(2-furyl)acryloyl]-L-leucine methyl ester (Fa-Leu-OMe) was flowed through the crystal at a concentration of 15 mM. Data were measured

to 2.0-Å resolution in 56% MeOH at −45 °C from a sorted list of intensities, with more counting time spent on the weaker reflections. Data collection and processing were accomplished as described for the native data. The initial phases were calculated using the coordinates of native elastase to 1.65-Å resolution in 56% MeOH at −45 °C. The final refinement results are given in Table 2.

(4) Attempted Formation of the Acyl-Enzyme at −26 °C in 56% MeOH. The substrate Fa-Leu-OMe was flowed through the crystal at a concentration of 15 mM. Data were measured to 2.0-Å resolution in 56% MeOH at −26 °C from a sorted list of intensities, with more counting time spent on the weaker reflections. Data collection and processing were accomplished as described for the native data. The initial phases were calculated using the coordinates of native elastase to 1.65-Å resolution in 56% MeOH at −45 °C. The final refinement results are given in Table 2.

(5) Attempted Formation of an Inhibitor Complex at −45 °C in 56% MeOH. 4′-Isopropyl-trifluoroacetyl-L-lysyl-L-phenylalaninanilide is a noncovalent inhibitor of elastase. It was flowed through the crystal at a concentration of 10^{-5} M (K_i = 4.4 × 10^{-7} M) (Renaud et al., 1983). Data were measured to 2.0-Å resolution in 56% MeOH at −45 °C from a sorted list of intensities, with more counting time spent on the weaker reflections. Data collection and processing were accomplished as described for the native data. The initial phases were calculated using the coordinates of native elastase to 1.65-Å resolution in 56% MeOH at −45 °C. The final refinement results are given in Table 2.

RESULTS AND DISCUSSION

Design of the Experiment. Fink and Ahmed (1976) conducted a series of kinetic studies of serine proteases at temperatures down to −70 °C in different aqueous–organic cryosolvents. At temperatures as low as −50 °C, the acyl-enzyme could be formed in solution, and the rate of deacylation was so slow that the intermediate was stable long enough for the collection of diffraction data. Although the acylation and deacylation rates for ZAP have not been determined at room temperature, the acylation rate for *p*-nitrophenyl trimethylacetate reacting with elastase has been reported (Bender & Marshall, 1968). The acylation rate at pH 7.5 and 25 °C is 2.2 × 10^{-3} s^{-1}, which is approximately the same as that for ZAP at pH 7.2 and −43.4 °C (1.1 × 10^{-3} s^{-1}) (Fink & Ahmed, 1976). The deacylation rate reported for the same ester substrate at 25 °C and pH 7.0 is 1.8 × 10^{-3} M s^{-1}. In comparison, the deacylation for ZAP occurs very slowly (1.2 × 10^{-10} mol s^{-1} at pH 7.2, −37 °C; Fink & Ahmed, 1976) at low temperature. These observations were used by Alber et al. (1976) in their 3.5-Å resolution X-ray crystallographic study of ZAP binding to porcine pancreatic elastase.

A control experiment reported as part of this study showed that raising the temperature to −10 °C allowed turnover of the trapped acyl-enzyme to occur (Douzou & Petsko, 1984). Since then, experiments by one of us (Rasmussen, unpublished) demonstrated that the crude low-temperature device used in the earlier 3.5-Å-resolution study (Alber et al., 1976) could not have produced a temperature as low as −55 °C at the crystal. A more likely value for the temperature attained was −35 °C. We therefore repeated the earlier 3.5-Å-resolution study at lower temperature—to stabilize the acyl-enzyme for the longer time needed for higher resolution data collection—with a new low-temperature device designed and constructed specifically for this project (Rasmussen, in preparation). In the first experiment, ZAP at −40 °C in 56% MeOH solvent at a concentration of 0.5 mM (this is the highest concentration possible so that ZAP will not precipitate at 56% MeOH cryosolvent, −40 °C) was flowed over the crystal. During the experiment, we performed continuous monitoring of the reflections that are known to change intensity when anything binds in the active site of the enzyme. No intensity changes were observed, indicating no binding of ZAP. We hypothesized that this negative result might be due to the low concentration of ZAP (K_M for this substrate at room temperature is about 0.6 mM) (Geneste & Bender, 1969) and possibly some reduction in the rate of both binding and catalysis on decreasing the temperature and changing the solvent. We then switched to the substrate *N*-[3-(2-furyl)acryloyl]-L-leucine methyl ester (Fa-Leu-OMe; K_M is estimated as 10 mM) since it is more soluble than ZAP in the 56% MeOH cryosolvent. A set of diffraction data to 2.0-Å resolution was collected at −45 °C in 56% MeOH cryosolvent with Fa-Leu-OMe at a concentration of 15 mM flowing over the crystal. The resulting electron density map indicated no binding of Fa-Leu-OMe. During this period, the intensities of reflections known to be sensitive to binding in the active site were continuously monitored. No intensity changes were observed (Figure 2).

Observations by ourselves and others (Morozov & Gevorkian et al., 1985; Frauenfelder & Gratton, 1986; Parak, 1986; Iben et al., 1989; Doster et al., 1986, 1989, 1991; Goldanskii et al., 1989; Champion, 1992) that proteins undergo a glass transition in their dynamic behavior at about −50 °C prompted us to investigate the effect of this transition on substrate binding. We found that crystalline ribonuclease A was not able to bind either specific substrates or inhibitors at temperatures below the glass transition, but that it could do so rapidly at higher temperatures (Rasmussen et al., 1992). Although an exhaustive study to establish the temperature of such a glass transition has not been done with PPE, the inability of PPE to react with substrates at −45 °C is a strong indication that such a transition exists in this temperature region. The presence of such a transition also predicts that an inhibitor will not bind to enzyme at −45 °C or lower temperatures either. To test this hypothesis, we flowed the inhibitor 4′-isopropyl-trifluoroacetyl-L-lysyl-L-phenylalaninanilide through the crystal. The structure of the complex formed between this inhibitor with elastase has been solved by Mattos et al. (1994). Data were collected to 2.0-Å resolution in 56% MeOH at −45 °C at a concentration of 10^{-5} M, which is about 100 K_i. During this period, the intensities of reflections known to be sensitive to binding in the active site were continuously monitored. No intensity changes were observed. The final refined electron density map indicated no binding of inhibitor, which is consistent with rigidification of the protein as an explanation for the failure of Fa-Leu-OMe binding to the protein at −45 °C.

These observations indicate that temperatures of −45 °C or below are too low for rapid formation of a complex to occur. Therefore, a higher temperature, well above the glass transition temperature, would seem to be required for reaction to occur. We chose the temperature −26 °C on the basis of observations made by Bartunik et al. (1992) in a series of crystallographic experiments. These investigators attempted to trap the acyl derivative formed by the reaction of PPE with the substrate Boc-Pro-Ala-Ala-OMe using time-resolved crystallography at a series of low temperatures starting at −53 and continuing up to −9 °C in steps of 5–10 K. At the lower temperatures, no changes in the diffraction pattern were observed. At around −23 °C, they saw a dramatic change in

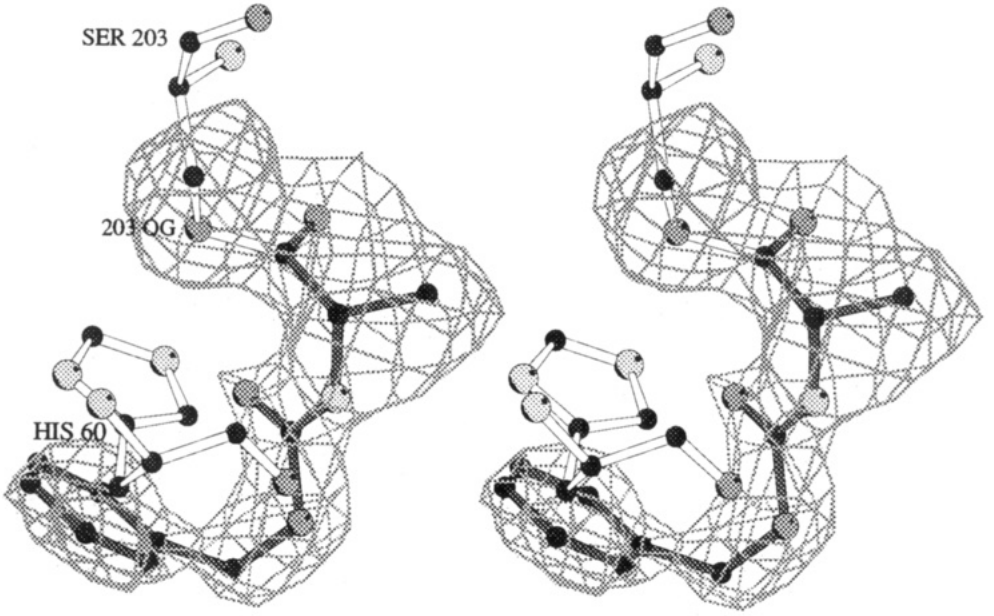

FIGURE 3: Final difference Fourier electron density map with coefficients ($|F_o| - |F_c|$). The map was calculated with a model from which the atoms of the side chains of serine 203(195) and the atoms of the substrate were omitted. Consequently, only the electron density corresponding to these atoms is showed. Superimposed on this electron density is the atomic model of the CBZ-Ala–elastase complex in the active site region, showing the atoms of Ser 203(195), His 60(57), and the bound substrate. The contour level for the electron density map is 1.7σ.

the diffraction patterns, which was interpreted as crystal disorder that might be caused by the formation of a Michaelis complex. The electron density maps calculated from the data obtained at –19 and –9 °C were interpreted as a mixture of the Michaelis complex and acyl-enzyme coexisting simultaneously on the enzyme. So we chose a temperature of around –23 °C for our work. A set of diffraction data to 2.0-Å resolution was collected at –26 °C in 56% MeOH cryosolvent with Fa-Leu-OMe at 15 mM flowing over the crystal. We saw intensity changes (Figure 2) consistent with those seen by Alber et al. (1976), but the final electron density map showed that no binding of substrate had occurred. This result indicates that, at –26 °C, the acyl-enzyme complex can be formed in the crystal, but a temperature of –26 °C is sufficiently high for turnover to occur, at least slowly. Our results from attempts to react substrates with PPE at various temperatures are exactly analogous with results obtained from ribonuclease A. Therefore, we assume that the same type of glass transition exists for PPE and that, under the conditions of our experiment, this glass transition temperature is around –45 °C. These results, plus the observations by Rasmussen et al. (1992) and Bartunik et al. (1992), led to the final strategy used to trap the acyl-enzyme intermediate successfully: formation of acyl-enzyme at –26 °C (a temperature above the glass transition) followed by a drop in the temperature to –55 °C (a temperature below the glass transition) to stabilize the acyl-enzyme intermediate.

Description of the Structure. PPE has two domains with the active site in the crevice between them. The active site, conserved for all serine proteases, consists of the catalytic triad [His 60(57), Asp 108(102), and Ser 203(195)], the oxyanion hole, and several subsites involved in the recognition and binding of substrate. In addition, in crystallographic structures of the native PPE, two sulfate ions are observed associated with the protein. One of them is in the active site region making hydrogen bonds with Oγ (2.7 Å) of Ser 203-(195), NE2 (2.8 Å) of His 60(57), and one water molecule, wat 369 (2.9 Å). The second sulfate ion is on the exterior of the protein, hydrogen bonded to NH1 (2.6 Å) of Arg 240-(230) and a water molecule (2.8 Å). There is also one calcium ion (CAL 280) found in PPE structures. This calcium ion has approximately octahedral coordination with six oxygen atoms [Glu 74(70) OE1, Glu 84(80) OE2, Asn 81(77) OD1, Asn 76(72) O, Gln 79(75) O, and a water molecule). In the CBZ-Ala–elastase complex reported here, the active site sulfate ion has been replaced by substrate. The exterior sulfate and calcium ions are still present.

Examination of the structure of the CBZ-Ala–elastase complex at 2.3-Å resolution reveals that the substrate ZAP has reacted with the active site Ser 203(195) and has formed a covalent bond with Oγ, as indicated by contiguous electron density between the carbonyl carbon of the alanine and the oxygen atom of Ser 203(195). The distance between these atoms in the final refined model is 1.5 Å. There is also clear electron density for the rest of the substrate, excluding the *p*-nitrophenolate leaving group. The model of bound substrate placed in the difference electron map is shown in Figure 3.

Compared to the native elastase structure at –45 °C, in 56% MeOH, the Ser 203 (195) Oγ of the complex structure has moved by a rotation of 20° about its CA–CB bond. At the same time, there is a movement of the imidazole ring of His 60(57) by a rotation of 13° about its CA–CB bond. This allows the NE2 of imidazole to form the same hydrogen bond with Oγ of Ser 203(195) (3.2 Å) as it does in the native structure (3.4 Å). There are no significant conformational changes in other parts of the enzyme upon formation of the complex. The root mean square difference between the complex and the native structure at –45 °C, 56% MeOH, is 0.23 Å for all backbone atoms (NCCO). This indicates that, in the acyl-enzyme, the protein has relaxed back to its initial conformation in the native enzyme structure, presumably after undergoing any needed conformational changes during the association–activation steps of substrate binding. Figure 4 shows the final refined structure of this acyl product bound to the enzyme. The carbonyl oxygen atom of alanine sits in the oxyanion hole, forming hydrogen bonds with the main chain NHs of both Gly 201(193) (2.5 Å) and Ser 203(195) (3.0 Å). The side chain methyl group is pointed away from the P1 pocket and is pointing toward the surface of the protein. The phenyl ring of the carbobenzoxy group of the substrate

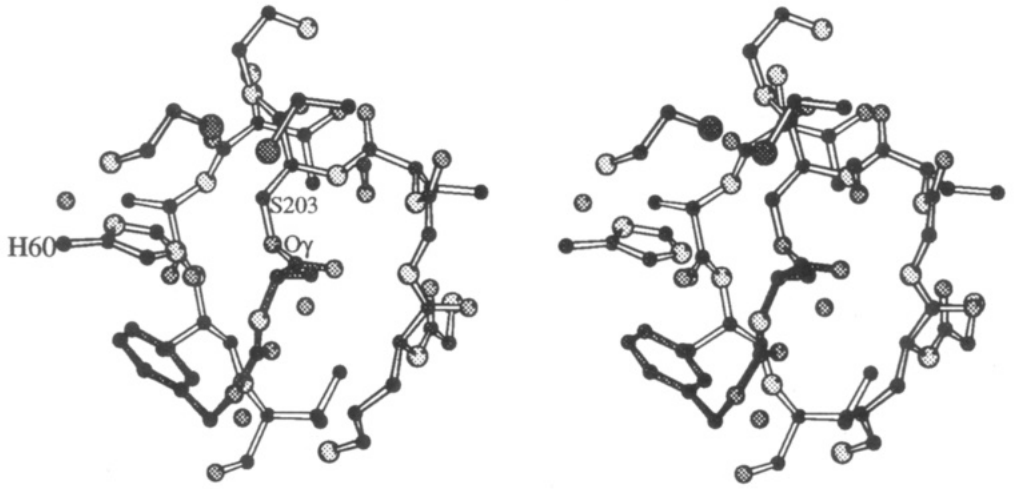

FIGURE 4: Stereoview of the acyl-enzyme intermediate in the active site of PPE. The substrate part is indicated by filled bonds, the protein by open bonds, and water molecules by circles.

binds in almost parallel fashion under His 60(57). The distance between the two aromatic planes is about 3.3 Å. It also lies in a good hydrophobic pocket formed by the Trp 98(94) ring system and the side chains of Phe 223(215) and Val 103(99). These interactions place the phenyl ring into the P2 pocket, in a position observed for hydrophobic groups in other elastase–inhibitor complexes (Mattos et al., 1994).

It has been proposed (Kraut, 1977) for the serine proteases that peptide substrates form the Michaelis complex with enzyme, with side chains occupying specific binding pockets in the active site region and the main chain atoms forming an antiparallel β-sheet with the protein. These interactions would position the carbonyl group of a substrate in a favorable position for nucleophilic attack at its carbonyl carbon by the oxygen of Ser 203(195). The ensuing tetrahedral intermediate then collapses to give the acyl-enzyme intermediate. It is assumed, if no large conformational changes occur in the substrate in going from the tetrahedral intermediate to the acyl-enzyme, that the acyl portion of the substrate should bind in the same way that it does in the Michaelis complex. Thus, the substrate should form an antiparallel β-sheet with backbone atoms of residues 222(214)–224(216), the side chains of the P residues interacting with the S subsites of the protein, and with the carbonyl oxygen positioned in the oxyanion hole. For the acyl-enzyme structure reported here, some of these expectations are observed and some are not.

For the CBZ-Ala–elastase complex, the carbonyl oxygen atom of alanine sits in the oxyanion hole forming hydrogen bonds with the main chain NHs of both Gly 201(193) and Ser 203(195). This arrangement should favor the formation of tetrahedral geometry for the carbon atom when it is attacked by water during the deacylation step, since it can stabilize the negative charge on the oxygen of the ensuing tetrahedral intermediate. These interactions also serve to polarize the carbonyl group in order to facilitate attack by nucleophilic water. The hydrogen bond distances observed in the acyl-enzyme complex can be compared to those reported for the structure of Ac-Ala-Pro-Val-difluoro-*N*-phenylethylacetamide bound to elastase (2.5 and 2.8 Å, respectively) (Takahashi et al., 1988). The inhibitor forms a stable complex with the enzyme by means of a covalent bond to Ser 203(195) Oγ, resulting in a hemiketal with tetrahedral geometry. This geometry is a mimic of the tetrahedral intermediate that forms immediately before and after formation of the acyl-enzyme.

The direction of binding of ZAP to elastase in the acyl-enzyme is in the direction of the S subsites. This orientation is believed to represent the productive, forward binding mode of a peptide bound to PPE. This orientation has been observed in the structure of Ac-Ala-Pro-Val-difluoro-*N*-phenylethylacetamide (Takahashi et al., 1989a) bound to elastase and in all peptide inhibitors bound to serine proteases other than elastase. It seems that the hydrophobic interaction of the phenyl ring of the substrate with the surrounding hydrophobic groups in the P2 site on the protein has dominated in orienting substrate binding. The strength of an interaction in the P2 pocket has been observed in the binding of a series of inhibitors to elastase (Mattos et al., 1994), in which the mode of binding changed dramatically in order to maintain this interaction. The CBZ-Ala–elastase structure was overlaid on the structure of Ac-Ala-Pro-Val-difluoro-*N*-phenylethylacetamide (Figure 5). In both cases, the P2 site is occupied by a hydrophobic group: benzene and proline, respectively. If this hydrophobic interaction is dominant in the binding of CBZ-Ala to the enzyme, then the rest of the molecule is pulled away from its ideal position, because an extra atom must be accommodated between the P2 pocket and the oxyanion hole. The result of positioning the benzene ring in the P2 pocket is that the whole substrate twists, pulling the side chain of alanine away from the P1 pocket. Elastase has broad specificity for peptides with small, uncharged, nonaromatic side chains, such as alanine residues (Geneste & Bender et al., 1970; Kaplan & Dugas, 1969). It has been proposed from kinetic studies (Thompson & Blout, 1970) that the increased reactivity of long-chain substrates is mostly due to an increase in the rate of the acylation. An efficient rate of acylation implies accurate orientation of the scissile bond relative to the catalytic residues. This orientation requires specific interactions with the protein to direct the positioning of the substrate. Small, hydrophobic side chains may not be very effective for this task, and positioning of the substrate therefore depends on backbone interactions. With a long peptide substrate or inhibitor, the backbone can make hydrogen bonds with the backbone of strand 222(214)–224(216), thereby directing the orientation and conformation. For instance, in the structure of PPE complexed with CBZ-Ala-Ile-boronic acid (Takahashi et al., 1989b), a hydrogen bond is observed between the NH of the P1 isoleucine and the carbonyl oxygen of Ser 222(214). The P2 and P3 residues do not form any hydrogen bonds. In contrast, in the structure of the PPE/Ac-Ala-Pro-Val-difluoro-*N*-phenylethylacetamide complex, the hydrogen bond between the NH of the P1 valine and the carbonyl oxygen of Ser 222-

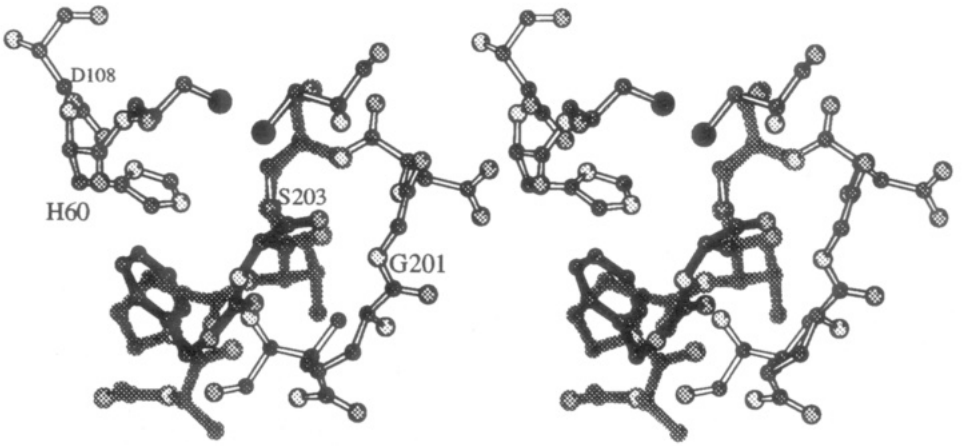

FIGURE 5: Superposition of ZAP and Ac-Ala-Pro-Val-difluoro-*N*-phenylethylacetamide (Takahashi et al., 1989b) bound to PPE. For the Ac-Ala-Pro-Val-difluoro-*N*-phenylethylacetamide structure, only the molecule bound in the region of ZAP is shown. The acyl-enzyme is shown in black bonds, the Ac-Ala-Pro-Val-difluoro-*N*-phenylethylacetamide in shaded bonds, and the protein in open bonds. The catalytic triad [H60(57), D108(102), and S203(195)] and G201(193) are labeled.

(214) is not observed. Instead, hydrogen bonds between the NH of the P3 alanine and the carbonyl oxygen of Val 224-(216) and between the carbonyl oxygen of the P3 alanine and the NH of Val 224(216) are observed. Therefore, we conclude that the hydrogen-bonding pattern observed with inhibitors is not always consistent.

In addition, the interactions that a small substrate such as ZAP can make with the protein may preclude the formation of the type of hydrogen bonds described here. This may be what happens with ZAP. With its short chain and one extra atom, the ZAP molecule is easily twisted. ZAP is, however, a better substrate than acetylalanine methyl ester or benzoylalanine methyl ester (Gertler & Hofmann, 1969), because of the added interactions between the CBZ phenyl ring and surrounding hydrophobic groups in the P2 site. In a model of the benzoyl-alanyl-PPE acyl-enzyme, the phenyl group of benzoylalanine cannot make these interactions because it cannot reach the site. The conclusions we can draw from our experiment are 2-fold: either the structure we observe is one in which the substrate binds nonproductively, or the conformation of the acyl-enzyme is productive and the enzyme can accommodate more than one type of binding mode in a productive turnover reaction. The facts that the carbonyl of the acyl-enzyme is stabilized by hydrogen bonds to the oxyanion hole and that the acyl-enzyme can hydrolyze at higher temperature (Douzou & Petsko, 1984) argue that this configuration is productive.

From a study of *Streptomyces griseus* protease A, James et al. (1980) have suggested that the acyl-enzyme of a serine protease is a high-energy ester with a pyramidal carbonyl carbon atom. They reason that a planar ester bond is chemically stable. They therefore suggest that a pyramidal arrangement, in which the oxygen is partially negatively charged and the carbonyl carbon is partially positively charged, stabilized by hydrogen bonding in the oxyanion hole, makes it a good electrophile for incoming water. In order to establish the geometry of the ZAP acyl derivative and to explore the possibility of a tetrahedral or partially tetrahedral geometry, we refined the structure of the carbonyl group with no geometric constraints. The planarity of the carbonyl group remained intact.

Singer et al. (1993) have discussed the location of a catalytic water molecule in their study of the acyl-enzyme complex formed by the reaction of trypsin with *p*-nitrophenyl guanidinobenzoate by time-resolved Laue crystallography. In their experiment, they treated trypsin with substrate at pH 5.5 and obtained Laue data before and shortly after initiating hydrolysis by jumping the pH to 8.5. A novel water molecule appearing at the higher pH was interpreted as a catalytic water that could act as a nucleophile in the deacylation step. In our study, no specific water molecule positioned to act as the attacking nucleophile is observed in the structure of the complex. Although we believe that the acyl-enzyme complex described here is representative of the productive acyl-enzyme in the turnover reaction of the substrate ZAP with PPE, this experiment is not designed to locate water molecules that could act as a nucleophile. Such a water molecule would have to be trapped along with the acyl group at the moment at which the tetrahedral intermediate is formed. Nevertheless, we believe that this low-temperature study provides a good model for the acyl-enzyme intermediate in the reaction of PPE with a small ester substrate, although it is not designed to trap intermediates of higher energy and shorter lifetime.

CONCLUSIONS

There are five possible intermediates on the reaction pathway of the serine proteases, as depicted in Figure 1. We have trapped and crystallographically characterized at high resolution the productive acyl-enzyme intermediate in the reaction of ZAP with elastase, thereby demonstrating that low-temperature protein crystallography can be used to trap productive intermediates along a reaction pathway under proper conditions.

REFERENCES

Alber, T., Petsko, G. A., & Tsernoglou, D. (1976) *Nature 263*, 297–300.

Bartunik, H. D., Bartunik, L. J., & Viehmann, H. (1992) *Philos. Trans. R. Soc. London. A 340*, 209–220.

Bender, M. L., & Marshall, T. H. (1968) *J. Am. Chem. Soc. 90*, 201–207.

Bender, M. L., & Killheffer, J. V. (1973) *CRC Crit. Rev. Biochem. 1*, 149–199.

Bernstein, F. C., Koetzle, T. F., Williams, G. J. B., Meyer, E. F., Jr., Brire, M. D., Rodgers, Y. R., Kenard, O., Shimanduchi, T., & Tasumi, M. (1977) *J. Mol. Biol. 112*, 535–542.

Blow, D. M. (1976) *Acc. Chem. Res. 9*, 145–152.

Brünger, A. T. (1988) *J. Mol. Biol. 203*, 803–816.

Brünger, A. T., Kuriyan, J., & Karplus, M. (1987) *Science 235*, 458–460.

Champion, P. M. (1992) *J. Raman Spectrosc. 23*, 557–567.

Doster, W., Bachleitner, A., Dunau, R., Hiebl, M., & Luscher, E. (1986) *Biophys. J. 50*, 213–219.
Doster, W., Cusack, S., & Petry, W. (1989) *Nature 337*, 754–756.
Doster, W., Cusack, S., & Petry, W. (1991) *J. Non-Cryst. Solids 131*, 357–361.
Douzou, P., & Petsko, G. A. (1984) *Adv. Protein Chem. 36*, 245–361.
Fink, A. L., & Ahmed, A. I. (1976) *Nature 263*, 294–297.
Frauenfelder, H., & Gratton, E. (1986) *Methods Enzymol. 127*, 207–216.
Geneste, P., & Bender, M. L. (1969) *Proc. Natl. Acad. Sci. U.S.A. 64*, 683–685.
Gertler, A., & Hofmann, T. (1969) *Can. J. Biochem. 48*, 384–386.
Goldanskii, V., & Krupyanskii, Y. F. (1989) *Q. Rev. Biophys. 22*, 39–92.
Hartley, B. S., & Kilby, B. A. (1954) *Biochem. J. 56*, 288–297.
Henderson, R. (1970) *J. Mol. Biol. 54*, 341–354.
Hendrickson, W. A., & Konnert, J. H. (1978) *Biomolecular structure, conformation, function and evolution: diffraction and related studies*, pp 43–57, Pergamon Press, Oxford, U.K.
Huber, R., & Bode, W. (1978) *Acc. Chem. Res. 11*, 114–121.
Iben, I. E. F., Braunstein, D., Doster, W., Frauenfelder, H., Hong, M. K., Johnson, J. B., Luck, S., Ormos, P., Schulte, A., Steinbach, P. J., Xie, A. H., & Young, R. D. (1989) *Phys. Rev. Lett. 62*, 1916–1919.
James, M. N. G., Sielecki, A. R., Brayer, G. D., & Delbaere, L. T. J. (1980) *J. Mol. Biol. 144*, 43–88.
Kaplan, H., & Dugas, H. (1969) *Biochem. Biophys. Res. Commun. 34*, 681.
Kaplan, H., Symonds, V. B., Dugas, H., & Whitaker, D. R. (1970) *Can. J. Biochem. 48*, 649.
Konnert, J. H., & Hendrickson, W. A. (1980) *Acta Crystallogr. A36*, 344–350.
Kraut, J. (1977) *Annu. Rev. Biochem. 46*, 331–358.
Mattos, C., Rasmussen, B. F., Ding, X. Ringe, D., & Petsko, A. P. (1994) *Nature Struct. Biol. 1*, 55–58.
Meyer, E., Cole, G., & Radhakrishnan, R. (1988) *Acta Crystallogr. B44*, 26–38.
Morozov, V. N., & Gevorkian, S. G. (1985) *Biopolymers 24*, 1785–1799.
Parak, F. (1986) *Methods Enzymol. 127*, 196–206.
Petsko, G. A. (1975) *J. Mol. Biol. 96*, 381–392.
Rasmussen, B. F., Stock, A. Ringe, D., & Petsko, G. A. (1992) *Nature 357*, 423–426.
Renaud, A., Lestienne, P., Hughes, D. L., Bieth, J. G., & Dimicoli, J. L. (1983) *J. Biol. Chem. 258*, 8312–8316.
Ringe, D., Mottonon, J. M., Gelb, M. H., & Abeles, R. H. (1986) *Biochemistry 25*, 5633–5639.
Ringe, D., Stoddard, B. L., Bruhnke, J., Koenigs, P., & Porter, N. (1992) *Philos. Trans. R. Soc. London A 340*, 273–284.
Sack, J. S. (1988) Documentation for PS300 Frodo-Molecular Graphics program for the PS300.
Sawyer, L. Shotton, D. M., Campbell, J. W., Wendell, P. L., Muirhead, H., Watson, H. C., Diamond, R., & Ladner, R. C. (1978) *J. Mol. Biol. 118*, 137–208.
Singer, P. T., Smalas, A., Carty, R. P., Mangel, W. F., & Sweet, R. M. (1993) *Science 259*, 669–673.
Stoddard, B. L., Bruhnke, J., Porter, N., Ringe, D., & Petsko, G. A. (1990) *Biochemistry 29*, 4871–4879.
Takahashi, L. H., Radhakrishnan, R., Rosenfield, R. E., Jr., Meyer, E. F., Jr., & Trainor, D. A. (1989a) *J. Am. Chem. Soc. 111*, 3368–3374.
Takahashi, L. H., Radhakrishnan, R., Rosenfield, R. E., Jr., & Meyer, E. F., Jr. (1989b) *Biochemistry 28*, 7610–7617.
Thompson, R. C., & Blout, E. R. (1970) *Proc. Natl. Acad. Sci. U.S.A. 67*, 1734–1740.
Turner, A. D., Pizzo, S. V., Rozakis, G., & Porter, N. A. (1987) *J. Am. Chem. Soc. 109*, 1274–1275.